Strain Mapping of Al–Mg Alloy with Multi-scale Grain Structure using Digital Image Correlation Method

B. Ahn*, S. R. Nutt
1. Department of Chemical Engineering and Materials Science, University of Southern California, Los Angeles, CA, 90089-0241, USA

*byungahn@usc.edu

Abstract: Al–Mg alloy powder was mechanically milled in liquid N_2 (cryomilling) to produce thermally stable powder with nanocrystalline (NC) microstructure for the manufacture of high-strength alloys. A multi-scale microstructure was achieved by blending unmilled coarse-grained (CG) powder with cryomilled powder and subsequently consolidating. The final bulk alloy was comprised of ultra-fine grained (UFG) regions and discrete CG bands. Dynamic observations of tensile deformation of the alloy were recorded using a micro-straining module attached to a light microscope, and the displacements were measured by digital image correlation (DIC). Strain inhomogeneity between UFG regions and ductile CG bands was observed in the micro-strain (strain order of 10^{-4}–10^{-6}) range, and the strain behavior was interpreted in terms of dislocation plasticity. Special emphasis was given to the distinct displacements between adjoining regions during deformation.

Key words: Digital image correlation-Strain mapping-Strain localization-Cryomilling-Ultrafine grains-Bimodal grain structures

1. Introduction

The great interest in nanostructured materials originates from the remarkably improved strength and potential for structural applications [1–3]. Cryomilling is one of several techniques to synthesize NC structures, such as mechanical alloying, high-pressure torsion, equal channel angular pressing, gas-phase condensation and electrodeposition. The merits of cryomilling include (a) cryogenic

Please cite this paper as: B. Ahn and S.R. Nutt, **"Strain mapping of Al-Mg alloy with multi-scale grain structure using digital image correlation method"** Experimental Mechanics 50 [1] (2009) 117-123 DOI **http://dx.doi.org/10.1007/s11340-008-9211-8**

temperature, which minimizes heat generation during milling so that recovery and recrystallization are suppressed, (b) rapid grain refinement and capability for production of large batches of refined powder (30–40 kg), (c) reduced oxygen contamination from the atmosphere, and (d) high thermal stability against grain growth because of large nitrogen content as a result of milling in liquid nitrogen [4–6]. However, bulk nanocrystalline materials often possess insufficient ductility and a reduced toughness compared to coarse-grained conventional materials. Multiple processing approaches have been employed to improve these properties [7–10]. In the present study, a novel approach analogous to ductile phase toughening was used to achieve a balance of high strength and acceptable toughness. Multi-scale grain structures were produced consisting of cryomilled NC regions and conventional CG regions. The resulting materials reportedly exhibit enhanced ductility compared to 100% NC materials, with only moderate strength decrements [11–13]. The deformation mechanisms in such multi-scale materials are not fully understood.

Some questions have arisen regarding the distribution of strain during plastic deformation of materials with discrete regions of two different grains sizes. The accurate measurements of local displacements and strains during deformation have been an important issue in the field of experimental mechanics. However, research trends toward reducing size scales to the micro/nanometer range give rise to difficulties when attempting to measure strains using conventional extensometry. In the case of non-uniform complex microstructures, such as the multi-scale structured material in the present study, conventional methods measure strains through the material without regard for the multi-scale microstructure, thus resulting in averaged strain values. DIC is a non-contacting displacement/strain field measuring technique offering the ability to analyze non-uniform full-field deformation. The DIC technique was first conceived a few decades ago and has been well developed recently to analyze and to visualize the actual strain distributions within

Please cite this paper as: B. Ahn and S.R. Nutt, **"Strain mapping of Al-Mg alloy with multi-scale grain structure using digital image correlation method"** Experimental Mechanics 50 [1] (2009) 117-123 DOI **http://dx.doi.org/10.1007/s11340-008-9211-8**

materials [14–17]. The basis of the DIC technique involves the mathematical tracking of numerical patterns consisting of different gray-scales of pixels between two digital images. In the 2-D DIC process, the correlation is carried out using a pair of sequential images under different loading conditions, then the surface displacements of the material can be precisely calculated by tracking movement of unique patterns in digital images of the microstructure. The DIC technique has proven to be an effective method for mapping displacements, and such a direct measurement method lends itself to development and validation of numerical or analytical models.

2. Experimental Procedures

2.1. Material Processing

Nanocrystalline powder was produced using mechanical attrition at a cryogenic temperature (cryomilling). Al 5083 (Al–4.4 Mg–0.7 Mn–0.15 Cr wt.%) gas-atomized alloy powder (<44 μm) was cryomilled in a 20 kg batch for 8 h with 6.4 mm stainless steel milling balls by DWA Aluminum Composites. The ball-to-powder weight ratio was 32:1, and 0.2 wt.% stearic acid was added as a processing control agent to improve the yield of powder and to moderate the cold welding process. Cryomilled NC powders were blended with 50 wt.% unmilled Al 5083 CG powder for multi-scale grain structure. Powder blends were loaded in aluminum cans for hot vacuum degassing at 450°C, then primarily compacted by cold isostatic pressing (CIP) at 310 MPa by Pittsburgh Materials Technology, Inc. The CIPped billet was quasi-isostatic forged two times by Advanced Materials & Manufacturing Technologies, LLC.

2.2. Mechanical Tests and Characterization

Uniaxial tensile deformation was performed at room temperature using a micro-tensile stage module (Deben UK Ltd.), as shown in Fig. 1(a). The module was designed for low displacement

Please cite this paper as: B. Ahn and S.R. Nutt, **"Strain mapping of Al-Mg alloy with multi-scale grain structure using digital image correlation method"** Experimental Mechanics 50 [1] (2009) 117-123 DOI **http://dx.doi.org/10.1007/s11340-008-9211-8**

rates (down to 300 nm/s), permitting micro-strain range deformation (minimum $4.18 \times 10{-}4$ s−1 strain rate in the present study). The tensile module was attached to a light microscope (Vanox AHMT3, Olympus), and the deformation during the tensile test was sequentially captured with time intervals of half a second using a digital camera (QICam, Qimaging) installed with the microscope. In order to facilitate dynamic observations of deformation, flat dog-bone tensile specimens were prepared with two notches to create an area of stress concentration. The gauge section was perpendicular to the forging direction with the dimensions of 4 mm (L) × 2.5 mm (W) × 1.5 mm (T), as shown in Fig. 1(b). The tensile specimen was finely polished and chemical-etched to facilitate observation of the multi-scale grain structure.

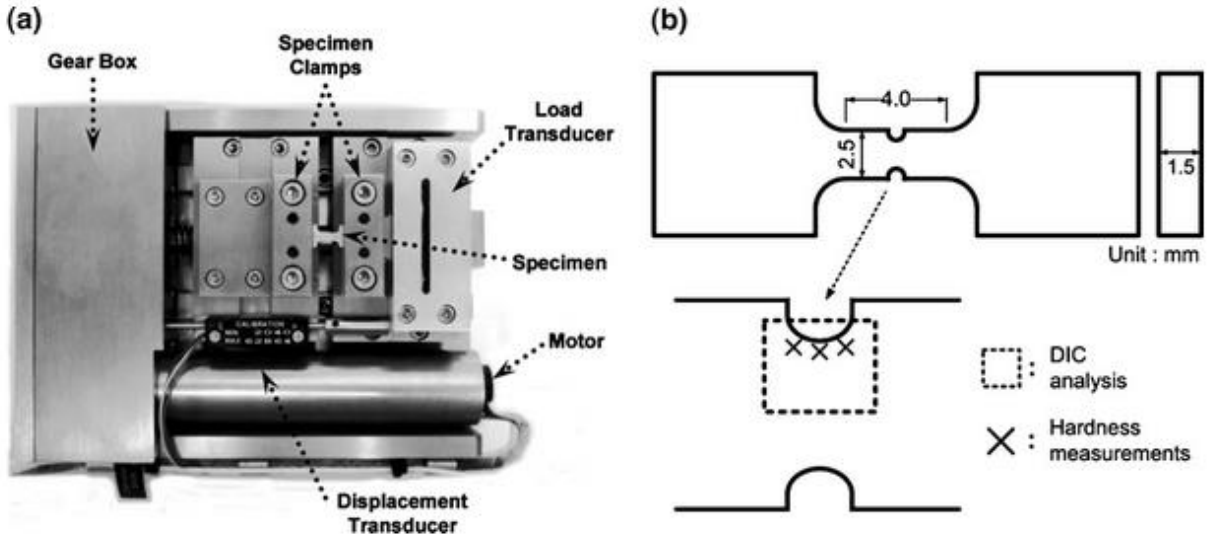

Fig. 1 (a) Micro-straining module to be attached to an optical microscopy: (b) geometry of a double-notched tensile specimen

The tensile test was interrupted for Vickers hardness (H_v) measurements at different stresses (182, 364, 455 and 515 MPa), and values were compared to initial hardness before the deformation. At each intermission, H_v was measured for both UFG and CG regions near a notch using a microhardness tester with a 10 gf load cell (Future-Tech Corp).

Please cite this paper as: B. Ahn and S.R. Nutt, **"Strain mapping of Al-Mg alloy with multi-scale grain structure using digital image correlation method"** Experimental Mechanics 50 [1] (2009) 117-123 DOI **http://dx.doi.org/10.1007/s11340-008-9211-8**

Microstructural characterization was conducted using both an optical microscope and a transmission electron microscope (Philips EM420 TEM) to investigate the multi-scale grain structure. TEM specimens were prepared by electrolytic twin jet polishing, and the number-based average grain size was measured directly from TEM images.

2.3. Digital Image Correlation (DIC)

To conduct the DIC analysis, pairs of micrographs were selected consisting of a reference image and a deformed state image recorded within a range of both large strain and micro-strain. DIC was performed to determine the displacement and strain field near a notch tip. The reference and deformed images were selected after yield of the material to correlate plastic strain only. The resolution of digital images was 1,392 × 1,040 pixels, and the corresponding field of view was 1,727 × 1,290 μm at low magnification for large strain and 434 × 324 μm at higher magnification for micro-strain measurements. Two-dimensional DIC was performed using software (VIC-2D, Correlated Solution, Inc). For suitable spatial resolution and reliable results of DIC, proper subset size and step size were selected. The pixel subset size should be selected large enough to encompass a unique pattern for the area of interest, but also small enough to distinguish strain differences in certain small regions. A large subset size would contain more distinctive patterns facilitating a reliable correlation analysis, but could cause an averaging effect on the strain field. On the other hand, the subset size must have a lower limit to minimize the influence of random noise. The step size controls the density of the analyzed data. A larger step size yields faster results but coarser data. In the present study, a subset size of 41 × 41 pixels and a step size of 4 pixels were used.

3. Results and Discussion

Please cite this paper as: B. Ahn and S.R. Nutt, **"Strain mapping of Al-Mg alloy with multi-scale grain structure using digital image correlation method"** Experimental Mechanics 50 [1] (2009) 117-123 DOI **http://dx.doi.org/10.1007/s11340-008-9211-8**

Figure 2 shows images of the as-forged microstructure, including a TEM dark field image and a light micrograph (inset). In the optical micrograph, regions of the UFG matrix (darker tone) and CG regions (brighter tone) are clearly observed. In general, CG regions were well dispersed in the UFG matrix showing evidence of dislocation activity during the forming processes. The multi-scale grain structure is apparent in the TEM dark field image in Fig. 2. The average grain size in the UFG matrix was ~240 nm, and ~4 μm for CG regions. Grains were generally non-equiaxed and were elongated perpendicular to the forging direction, as shown in Fig. 2. The cryomilled powder exhibited an average equiaxed grain size of 50 nm prior to consolidation with a narrow size distribution as reported previously [18]. However, moderate grain growth occurred during high temperature processing (hot degassing and forging), resulting in an UFG structure.

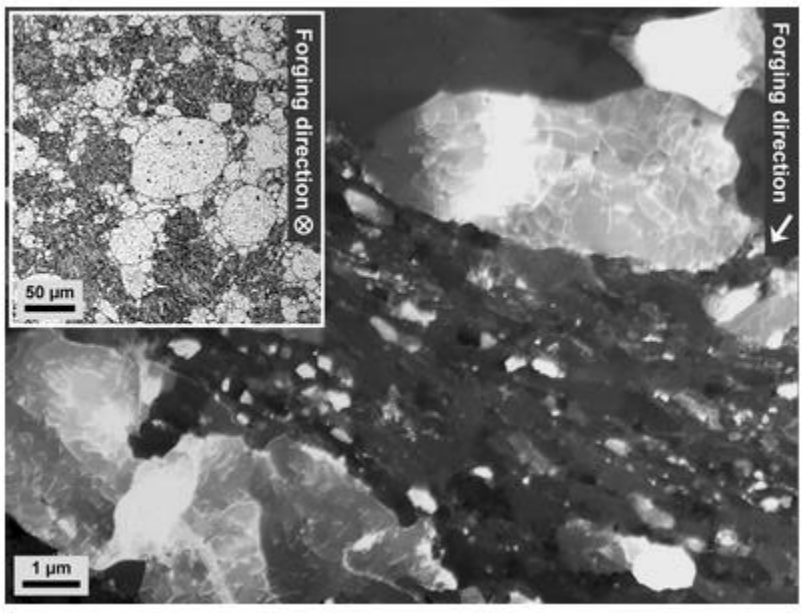

Fig. 2 TEM dark field image and optical micrograph of multi-scale grain structures

The tensile properties of the as-forged material with multi-scale grain structures are shown in Table 1, and compared with cryomilled 100% NC material and conventional 100% CG material.

Please cite this paper as: B. Ahn and S.R. Nutt, **"Strain mapping of Al-Mg alloy with multi-scale grain structure using digital image correlation method"** Experimental Mechanics 50 [1] (2009) 117-123 DOI **http://dx.doi.org/10.1007/s11340-008-9211-8**

The yield strength of a notched specimen in the direction normal to the forging direction was 265 MPa, almost twice the strength of Al 5083 alloy with conventional grain size (145 MPa) [11]. The tensile elongation (5.5%) of this bimodal grain structured materials (50% NC + 50% CG) was also four times greater than that of cryomilled 100% NC material (1.4%) [11].

Table 1 Tensile properties of a multi-scale grain structured material compared with two uniform grain-sized materials [11]

Materials	Yield strength (MPa)	UTS (MPa)	Elongation (%)
100% NC [10]	641	847	1.4
50% NC + 50% CG	265	524	5.5
100% CG [10]	145	281	16

Figure 3 shows a selected sequence of images of deformation and fracture around a notch during a tensile test. Figure 3(a) is an initial image before the deformation. The images of deformed material, Fig. 3(b)–(d), were selected from different stages of deformation, 60, 100 and 110 s after Fig. 3(a), which are equivalent to total strains of $2.51 \times 10{-}2$, $4.18 \times 10{-}2$ and $4.59 \times 10{-}2$, respectively. Figure 3(b) shows that micro-voids and micro-cracks started to nucleate at the root of a notch short time after the material yielded. In Fig. 3(c), the micro-cracks grew and coalesced, forming a network. Finally, the network expanded rapidly toward the center of the specimen, developing macro-cracks and resulting in material rupture, as shown in Fig. 3(d). Prior to failure, no significant area reduction was observed in the gage section.

Please cite this paper as: B. Ahn and S.R. Nutt, **"Strain mapping of Al-Mg alloy with multi-scale grain structure using digital image correlation method"** Experimental Mechanics 50 [1] (2009) 117-123 DOI **http://dx.doi.org/10.1007/s11340-008-9211-8**

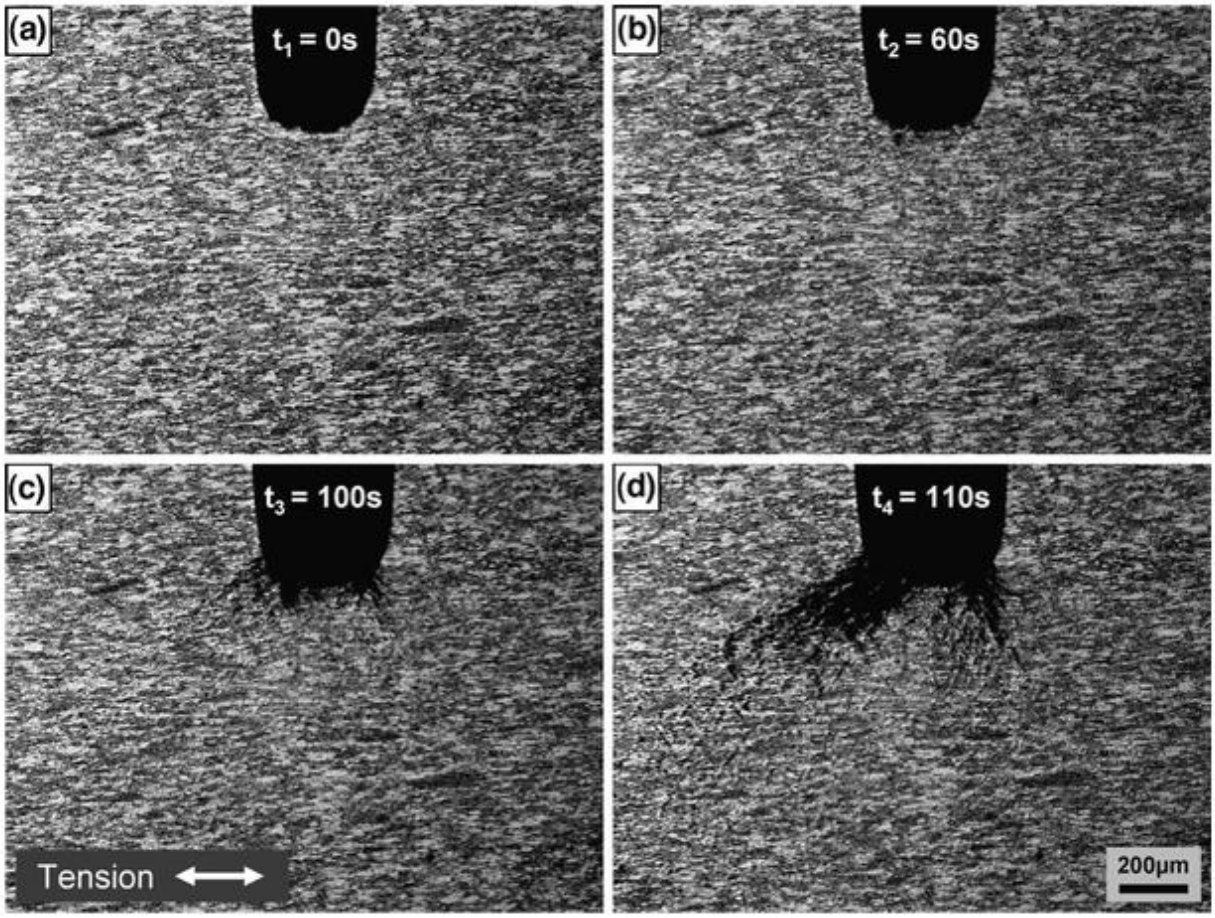

*Fig. 3 Successive optical micrographs recorded around a notch during tensile deformation; (**a**) initial state before deformation started ($t_1 = 0$ s); (**b**) voids nucleated short time after yielding ($t_2 = 80$ s); (**c**) fracture started ($t_3 = 100$ s); (**d**) immediately before rupture of the specimen ($t_4 = 110$ s)*

The strain field measured by DIC for three different time intervals is shown in Fig. 4. Strain evolution during the deformation is readily apparent. In Fig. 4(a), DIC was employed for a 30-s interval (1.25 × 10−2 strain) between the reference and deformed images. The correlation shows that the maximum strain occurred in front of the notch tip as a result of the stress concentration. Also, strain localization is apparent at orientations of approximately 45° to the tension axis, where the resolved shear stress is a maximum, generating a gradient toward the center of the specimen. When DIC was performed for a 6-s interval (2.51 × 10−3 strain) as shown in Fig. 4(b), the magnitude of

Please cite this paper as: B. Ahn and S.R. Nutt, **"Strain mapping of Al-Mg alloy with multi-scale grain structure using digital image correlation method"** Experimental Mechanics 50 [1] (2009) 117-123 DOI **http://dx.doi.org/10.1007/s11340-008-9211-8**

strain was significantly decreased compared with Fig. 4(a). No distinct strain variation was observed between UFG and CG regions in Fig. 4(b). However, when two images in a very small strain range of 1 s interval (4.18 × 10−4 strain) were correlated, slight strain localization was observed, manifest as scattered spots in Fig. 4(c). The strain localization was attributed to different deformation behavior of UFG and CG regions. However, the resolution of the DIC results in Fig. 4 was insufficient to provide detailed evidence of the local strain distribution with respect to the multi-scale grain structure.

According to the Hall–Petch relation, the yield strength is inversely proportional to grain size. When dislocations encounter obstacles (e.g. grain boundaries), the mobility of dislocations decreases, causing an increase in the stress required to continue deformation. Indeed, CG regions with ~4 μm grain size are relatively softer than UFG regions with ~240 nm grain size. Therefore, within CG regions, more dislocations are generated and their mobility is greater because of the lower density of obstacles (e.g. grain boundaries) in the larger grains. Conversely, the mobility of dislocations within harder UFG regions is limited because of the smaller grains. Nevertheless, the strain inhomogeneity between UFG and CG regions apparent in the DIC results at micro-strain was ultimately accommodated, since the total strain within the material must be continuous through both UFG and CG regions.

Please cite this paper as: B. Ahn and S.R. Nutt, **"Strain mapping of Al-Mg alloy with multi-scale grain structure using digital image correlation method"** Experimental Mechanics 50 [1] (2009) 117-123 DOI **http://dx.doi.org/10.1007/s11340-008-9211-8**

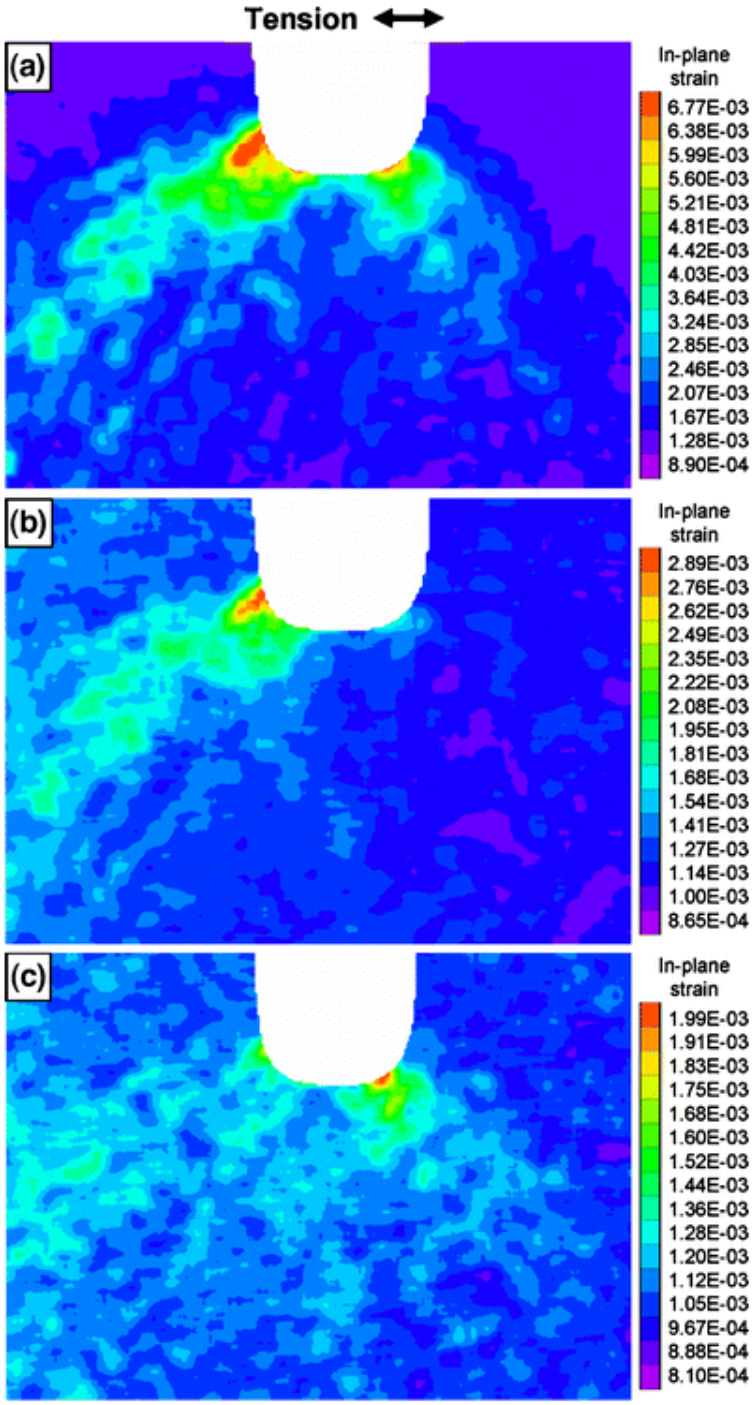

Fig. 4 In-plane strain fields around a notch measured by DIC at different strains; (a) large strain (1.25×10^{-2}, 30 s interval); (b) intermediate strain (2.51×10^{-3} strain, 6 s interval); (c) micro-strain (4.18×10^{-4}, 1 s interval)

Please cite this paper as: B. Ahn and S.R. Nutt, **"Strain mapping of Al-Mg alloy with multi-scale grain structure using digital image correlation method"** Experimental Mechanics 50 [1] (2009) 117-123 DOI **http://dx.doi.org/10.1007/s11340-008-9211-8**

Despite the accommodation of local strain differences, different deformation mechanisms are expected in the UFG regions. As discussed above, dislocation plasticity is limited in UFG regions compared to CG regions. However, grain boundary mediated plasticity, such as grain boundary sliding and grain rotation, is also less likely in the grain size of ~240 nm especially at room temperature. The initiation and evolution of micro-cracks in UFG regions or at interfaces between UFG and CG regions may occur to compensate the plastic strain in CG regions and accommodate strain inhomogeneity. Concurrently, the initiation and fast propagation of cracks through UFG regions can be delayed by plastic deformation and crack blunting in CG regions. In general, voids/cracks are expected to initiate and grow from existing defects in the materials, such as porosity or poor interparticle boundaries.

Figure 6 shows a DIC result when porosity exist at the boundary between UFG and CG regions. Two images were selected for the DIC analysis, also taken at half-second intervals (~2.09×10^{-4} strain) after yielding. The porosity is illustrated as blue circles in the reference image shown in Fig. 6(a), and the corresponding micro-strain contour is shown in Fig. 6(b). The red arrows in Fig. 6(b) indicate regions in which the strain is highly concentrated, and the corresponding regions are indicated by similar red arrows in Fig. 6(a). The strain is concentrated in CG regions adjacent to the pores, indicative of greater plastic deformation and relaxation of the stress concentration at the pores.

Please cite this paper as: B. Ahn and S.R. Nutt, **"Strain mapping of Al-Mg alloy with multi-scale grain structure using digital image correlation method"** Experimental Mechanics 50 [1] (2009) 117-123 DOI **http://dx.doi.org/10.1007/s11340-008-9211-8**

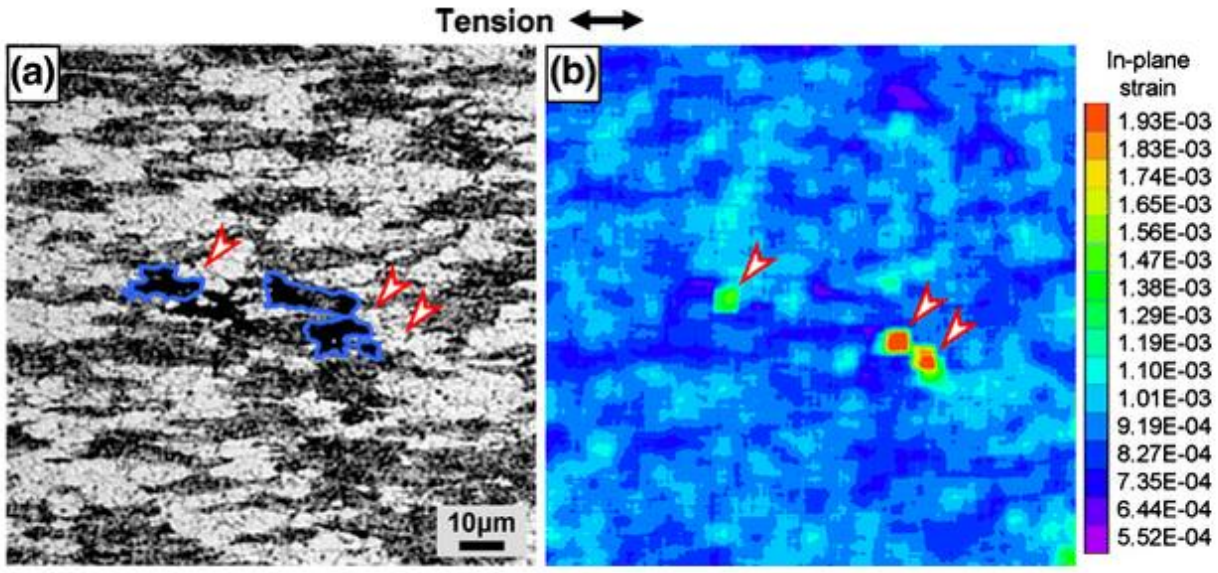

Fig. 6 (a) Optical micrograph and (b) corresponding in-plane strain field showing strain concentration in CG regions adjacent to porosity

The phenomenon of plastic strain concentration in CG regions was consistent with values of Vickers hardness (H v) measured near the notch both in UFG and CG regions. The H v was measured before the tensile test (0 MPa) and at four intermissions (182, 364, 455 and 515 MPa) during the deformation, as shown in Fig. 7. Both in UFG and CG regions, the H v increased after yielding (265 MPa). The H v of CG regions increased ~30% after significant plastic strain, while the increment in UFG regions was only ~5%. The hardness results were consistent with strain localization revealed by strain mapping using the DIC technique, described above. During tensile deformation, the CG regions underwent greater strain-hardening compared to the UFG regions, and it is due to the increase in dislocation density and the mutual interaction between dislocations. After the material yielded, the dislocation density increased significantly in CG regions, as shown in Fig. 8. Dislocations accumulate, interact, and serve as pinning points or obstacles that significantly impede glide. The enhanced ductility in this multi-scale grain structured material compared with 100% NC/UFG materials is attributed to the greater increase in dislocation mobility in CG regions in which

Please cite this paper as: B. Ahn and S.R. Nutt, **"Strain mapping of Al-Mg alloy with multi-scale grain structure using digital image correlation method"** Experimental Mechanics 50 [1] (2009) 117-123 DOI **http://dx.doi.org/10.1007/s11340-008-9211-8**

dislocations glide more easily on slip systems. The material is strain-hardened by tangles of dislocations, and is toughened against abrupt brittle failure through UFG regions.

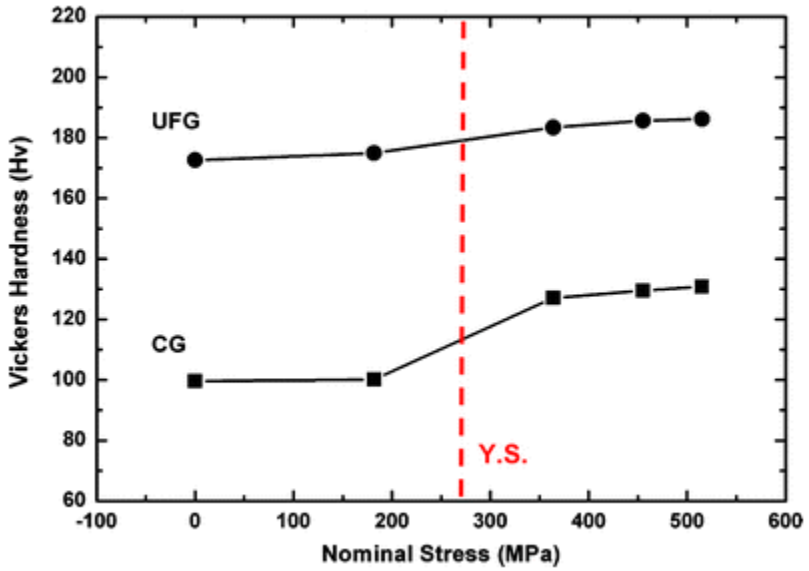

Fig. 7 Variation of Vickers hardness measured from both UFG and CG regions near a notch during tensile deformation

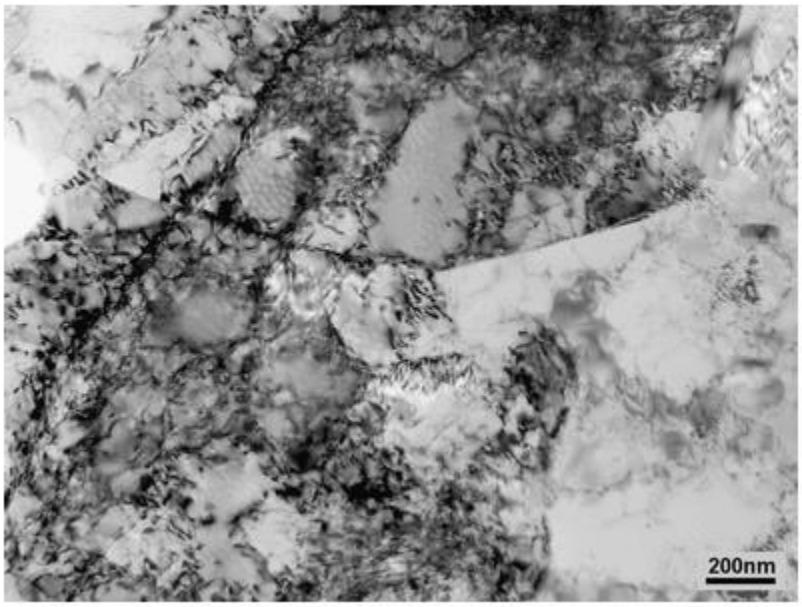

Fig. 8 Dislocation structures in CG regions produced by plastic deformation in tension. Denser tangles of dislocations are apparent, compared to the as-consolidated state in Fig. 2

4. Conclusions

Please cite this paper as: B. Ahn and S.R. Nutt, **"Strain mapping of Al-Mg alloy with multi-scale grain structure using digital image correlation method"** Experimental Mechanics 50 [1] (2009) 117-123 DOI **http://dx.doi.org/10.1007/s11340-008-9211-8**

Strain distribution in multi-scale grain structures was observed during tensile deformation. Strain evolution was successfully measured by DIC, and full-field strain mapping was demonstrated for this bimodal microstructure. Inhomogeneous strain was observed in UFG and CG regions, and the deformation was correlated in micro-strain range. The strain was localized in CG regions, primarily because of greater dislocation plasticity in these regions compared to UFG regions. DIC showed that, in the presence of porosity at CG-UFG interfaces, CG regions adjacent to the porosity resisted fast delamination of two regions. The localized strain in CG regions was explained by hardness variations, which showed that more strain hardening occurred in CG regions during plastic deformation. This phenomenon arose from the increase in dislocation density in CG regions compared to UFG regions. Strain mapping performed by DIC offers insights into strain distribution within the microstructure. Future work will address the evolution of strain distribution with respect to CG fraction in bimodal structures.

Acknowledgements: Financial support was provided by the Army Research Office under contract W911NF-08-2-0028. The authors gratefully acknowledge Prof. Enrique J. Lavernia (University of California, Davis) for providing materials and professional advice, and Prof. Kwang Ho Kim (National Core Research Center for Hybrid Materials Solution, Busan, Korea) for valuable technical discussions. A trial license of the VIC-2D software from the Correlated Solution, Inc. is particularly appreciated.

References:

1. Gleiter H (1989) Nanocrystalline materials. Prog Mater Sci 33:223–315 doi: 10.1016/0079-6425(89)90001-7
2. Weertman JR, Averback RS (1996) Mechanical properties. In: Edelstein AS, Cammarata RC (eds) Nanomaterials: synthesis, properties and applications. Institute of Physics Publishing, Bristol, pp 323–345

Please cite this paper as: B. Ahn and S.R. Nutt, **"Strain mapping of Al-Mg alloy with multi-scale grain structure using digital image correlation method"** Experimental Mechanics 50 [1] (2009) 117-123 DOI **http://dx.doi.org/10.1007/s11340-008-9211-8**

3. Newbery AP, Han BQ, Lavernia EJ, Suryanarayana C, Christodoulou JA (2007) Mechanical alloying and severe plastic deformation. In: Groza JR, Shackelford JF, Lavernia EJ, Powers MT (eds) Materials processing handbook. CRC, Boca Raton, FA, pp 13.1–13.28
4. Perez RJ, Huang B, Lavernia EJ (1996) Thermal stability of nanocrystalline Fe–10 wt.% Al produced by cryogenic mechanical alloying. Nanostruct Mater 7:565–572 doi: 10.1016/0965-9773 (96)00020-7
5. Perez RJ, Jiang HG, Dogan CP, Lavernia EJ (1998) Grain growth of nanocrystalline cryomilled Fe–Al powders. Metall Mater Trans 29A:2469–2475 doi: 10.1007/s11661-998-0218-7
6. Witkin DB, Lavernia EJ (2006) Synthesis and mechanical behavior of nanostructured materials via cryomilling. Prog Mater Sci 51:1–60 doi:10.1016/j.pmatsci.2005.04.004
7. Wang Y, Chen M, Zhou F, Ma E (2002) High tensile ductility in a nanostructured metal. Nature 419:912–915 doi: 10.1038/nature01133
8. He G, Eckert J, Löser W, Schultz L (2002) Novel Ti-base nanostructure-dendrite composite with enhanced plasticity. Nat Mater 2:33–37 doi: 10.1038/nmat792
9. Tellkamp VL, Melmed A, Lavernia EJ (2001) Mechanical behavior and microstructure of a thermally stable bulk nanostructured Al alloy. Metall Mater Trans 32A:2335–2343 doi: 10.1007/s11661-001-0207-6
10. Youssef KM, Scattergood RO, Murty KL, Koch CC (2006) Nanocrystalline Al–Mg alloy with ultrahigh strength and good ductility. Scr Mater 54:251–256 doi:10.1016/j.scriptamat.2005.09.028
11. Witkin D, Lee Z, Rodriguez R, Nutt R, Lavernia E (2003) Al–Mg alloy engineered with bimodal grain size for high strength and increased ductility. Scr Mater 49:297–302 doi: 10.1016/S1359-6462(03)00283-5
12. Han BQ, Lee Z, Witkin D, Nutt S, Lavernia EJ (2005) Deformation behavior of bimodal nanostructured 5083 Al alloys. Metall Mater Trans 36A:957–965 doi: 10.1007/s11661-005-0289-7
13. Lee Z, Witkin DB, Radmilovic V, Lavernia EJ, Nutt SR (2005) Bimodal microstructure and deformation of cryomilled bulk nanocrystalline Al–7.5 Mg alloy. Mater Sci Eng A 410–411:462–467 doi: 10.1016/j.msea.2005.08.104
14. Chu TC, Ranson WF, Sutton MA, Peters WH (1985) Application of digital-image-correlation techniques to experimental mechanics. Exp Mech 25:232–244 doi: 10.1007/BF02325092
15. Bruck HA, McNeill SR, Sutton MA, Peters WH (1989) Digital image correlation using Newton–Raphson method of partial differential correction. Exp Mech 29:261–267 doi: 10.1007/ BF02321405
16. James MR, Morris WL, Cox BN (1990) A high-accuracy automated strain-field mapper. Exp Mech 30:60–67 doi: 10.1007/ BF02322704
17. Smith BW, Li X, Tong W (1989) Error assessment for strain mapping by digital image correlation. Exp Tech 22:19–21 doi:10.1111/j.1747-1567.1998.tb02332.x
18. Ahn B, Newbery AP, Lavernia EJ, Nutt SR (2007) Effect of degassing temperature on the microstructure of a nanocrystalline Al–Mg alloy. Mater Sci Eng A 463:61–66 doi: 10.1016/j.msea.2006.07.158

Please cite this paper as: B. Ahn and S.R. Nutt, **"Strain mapping of Al-Mg alloy with multi-scale grain structure using digital image correlation method"** Experimental Mechanics 50 [1] (2009) 117-123 DOI **http://dx.doi.org/10.1007/s11340-008-9211-8**